




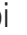









Original research

Diffusion-based structural connectivity patterns of multiple sclerosis phenotypes

Eloy Martinez-Heras ¹, Elisabeth Solana,¹ Francesc Vivó,¹ Elisabet Lopez-Soley,¹ Alberto Calvi ¹, Salut Alba-Arbalat,¹ Menno M Schoonheim ², Eva M Strijbis ³, Hugo Vrenken,⁴ Frederik Barkhof,^{4,5} Maria A Rocca ^{6,7,8}, Massimo Filippi ^{6,7,8,9}, Elisabetta Pagani,⁶ Sergiu Groppa ¹⁰, Vinzenz Fleischer ¹⁰, Robert A Dineen ¹¹, Barbara Bellenberg,¹² Carsten Lukas,¹² Deborah Pareto,¹³ Alex Rovira ¹³, Jaume Sastre-Garriga ¹⁴, Sara Collorone ¹⁵, Ferran Prados,^{15,16,17} Ahmed Toosy,¹⁵ Olga Ciccarelli,¹⁵ Albert Saiz,¹ Yolanda Blanco,¹ Sara Llufriu ¹

► Additional supplemental material is published online only. To view, please visit the journal online (<http://dx.doi.org/10.1136/jnnp-2023-331531>).

For numbered affiliations see end of article.

Correspondence to

Dr Sara Llufriu, Neuroimmunology and Multiple Sclerosis Unit and Laboratory of Advanced Imaging in Neuroimmunological Diseases (ImaginEM), IDIBAPS, Barcelona 08036, Spain; SLLUFRIU@clinic.cat

Received 27 March 2023
Accepted 30 May 2023



© Author(s) (or their employer(s)) 2023. No commercial re-use. See rights and permissions. Published by BMJ.

To cite: Martinez-Heras E, Solana E, Vivó F, et al. *J Neurol Neurosurg Psychiatry* Epub ahead of print: [please include Day Month Year]. doi:10.1136/jnnp-2023-331531

ABSTRACT

Background We aimed to describe the severity of the changes in brain diffusion-based connectivity as multiple sclerosis (MS) progresses and the microstructural characteristics of these networks that are associated with distinct MS phenotypes.

Methods Clinical information and brain MRIs were collected from 221 healthy individuals and 823 people with MS at 8 MAGNIMS centres. The patients were divided into four clinical phenotypes: clinically isolated syndrome, relapsing-remitting, secondary progressive and primary progressive. Advanced tractography methods were used to obtain connectivity matrices. Then, differences in whole-brain and nodal graph-derived measures, and in the fractional anisotropy of connections between groups were analysed. Support vector machine algorithms were used to classify groups.

Results Clinically isolated syndrome and relapsing-remitting patients shared similar network changes relative to controls. However, most global and local network properties differed in secondary progressive patients compared with the other groups, with lower fractional anisotropy in most connections. Primary progressive participants had fewer differences in global and local graph measures compared with clinically isolated syndrome and relapsing-remitting patients, and reductions in fractional anisotropy were only evident for a few connections. The accuracy of support vector machine to discriminate patients from healthy controls based on connection was 81%, and ranged between 64% and 74% in distinguishing among the clinical phenotypes.

Conclusions In conclusion, brain connectivity is disrupted in MS and has differential patterns according to the phenotype. Secondary progressive is associated with more widespread changes in connectivity. Additionally, classification tasks can distinguish between MS types, with subcortical connections being the most important factor.

INTRODUCTION

Multiple sclerosis (MS) is a chronic inflammatory, demyelinating and neurodegenerative disorder of the central nervous system, which is characterised by varying degrees of physical and cognitive

WHAT IS ALREADY KNOWN ON THIS TOPIC

- ⇒ Multiple sclerosis (MS) is a neurodegenerative disease characterised by inflammation and demyelination in the central nervous system, leading to disrupted neural connections and varying clinical phenotypes.
- ⇒ People with MS present disconnection of brain networks, mainly due to poor integration between cortical areas and enhanced segregation of brain regions.
- ⇒ Diffusion-based MRI techniques and graph theory can be used to study microstructural changes and brain network alterations in patients with MS across different phenotypes.

WHAT THIS STUDY ADDS

- ⇒ The study highlights distinct patterns of brain connectivity disruptions associated with different MS phenotypes, particularly revealing more widespread changes in connectivity for secondary progressive MS.
- ⇒ It demonstrates the effectiveness of support vector machine algorithms in classifying patients from healthy controls (81% accuracy) and distinguishing among clinical phenotypes (64% to 74% accuracy) based on brain connectivity patterns.
- ⇒ The study emphasises the importance of subcortical connections as a key factor in differentiating MS types, providing valuable insights into the underlying neural mechanisms related to MS phenotypes.

HOW THIS STUDY MIGHT AFFECT RESEARCH, PRACTICE OR POLICY

- ⇒ This study might affect research, practice or policy by providing a better understanding of the differential patterns of brain connectivity disruptions across MS phenotypes, which can guide the development of more accurate diagnostic and prognostic tools, leading to improved personalised treatment and management strategies for people with MS.

disability.¹ The diversity in the progression of the disease has been traditionally classified into several phenotypes: patients with a clinically isolated syndrome (CIS), commonly progressing to a relapsing-remitting MS (RRMS) disease course and eventually, experiencing a poorly understood sustained deterioration in their disability independent of relapses after several years, referred to as secondary progressive MS (SPMS). In addition, a smaller percentage of patients develop a progressive course from the very beginning, known as primary progressive MS (PPMS).²

MS is characterised by the presence of focal and diffuse damage within the white and grey matter (GM) of the brain,³ which accumulates as the disease progresses and disrupts structural connections in the brain.⁴ Diffusion magnetic resonance imaging (MRI) can offer information regarding the integrity of white matter (WM) connections, representing the topology and hierarchy of structural brain networks.⁵ The disconnection among MS brain networks is characterised by impaired information flow and worse network efficiency, mainly due to poor integration between cortical areas and the enhanced segregation of brain regions.⁶ In particular, long-range anatomical tracts are damaged, and at later stages of the disease the disruption of the connections between network hubs becomes more prominent.⁷ The changes in networks are quite heterogeneous in MS, depending mainly on the areas damaged and the severity of the disruptions.^{8,9} In fact, compensatory reorganisation can to some extent preserve the global efficiency of the brain in the early stages of the disease, mainly manifested by functional changes.¹⁰ By contrast, at more advanced stages of MS, structural damage leads to less efficient network wiring and when this loss of efficiency reaches a critical threshold, the network collapses and clinical progression accelerates.¹¹

At present, the extent and characteristics of the modifications in structural connectivity in relation to MS phenotypes are not well understood. A previous report found differences in global and local network metrics between RRMS and SPMS, that seemed partially independent of the disconnection effects of focal lesions.¹² Hence, it would appear that those previous results of an overall decline in network integrity were caused principally by the effects of lesion load on the underlying tissue structure. Preliminary studies that employed machine learning (ML) algorithms and binary classifications to discriminate clinical phenotypes based on the characteristics of connectivity displayed good accuracy, suggesting that the distinct MS phenotypes are associated with different network modifications,^{13,14} but this awaits confirmation in larger samples.

Here, we set out to comprehensively test the clinical relevance of structural network changes in MS by describing the modifications to brain networks and their components associated with the different MS phenotypes, and to assess the ability of these modifications to classify the changes in connectivity. To this end, we studied a large cohort of people with MS (PwMS) recruited through a multicentre collaboration within the MAGNIMS network.

METHODS

Participants

In this retrospective cross-sectional study, we included data from eight centres across Europe that were members of the MAGNIMS network (<https://www.magnims.eu/>): (1) ImaginEM group at the Hospital Clinic Barcelona (Spain); (2) The Amsterdam MS Center, Amsterdam UMC, location VUmc, Amsterdam (The Netherlands); (3) The Neuroimaging Research Unit, San Raffaele Scientific Institute, Milan (Italy); (4) University Medical

Center of the Johannes Gutenberg University Mainz (Germany); (5) Division of Clinical Neuroscience, University of Nottingham, Nottingham (UK); (6) St. Josef Hospital Ruhr University, Bochum (Germany); (7) The Cemcat and Section of Neuroradiology, University Hospital Vall d'Hebron, Barcelona (Spain); and (8) Institute of Neurology, UCL, London (UK). None of the participants had any clinically signs of relapse nor had they received steroid treatment in the 30 days prior to the study visit. The MRI scans, obtained from the participants during the period from 2011 to 2019, were incorporated into our analysis. After conducting a quality-control evaluation, we excluded 27 PwMS due to poor alignment between MRI modalities, despite the quality of the data meeting our standards (see the MRI acquisition and processing section). We then proceeded to analyse the clinical and demographic information of the final cohort, which consisted of 823 PwMS according to 2010 McDonald criteria and 221 healthy controls (HCs). Patients with a CIS presented radiological dissemination in space, while SPMS participants had a progressive accumulation of neurological disability over at least 1 year after a relapsing remitting phase.

Data transfer agreements were established with the participating centres in order to allow sharing of pseudonymised images and clinical information governed by a central MAGNIMS collaboration framework agreement.

Magnetic resonance acquisition and processing

MRI scans were collected for each participant site using 3T scanners (different vendors) using common MRI acquisition parameters (MRI details for each centre are provided in online supplemental table 1): (A) 3D-T1 structural sequences with ≤ 1.5 mm isotropic voxel size and (B) whole brain diffusion scans with at least 30 diffusion encoding directions, ≤ 2.5 mm isotropic voxel size and b value ≥ 900 s/mm². We computed whole brain and local (nodal) graph metrics, as well as the fractional anisotropy (FA) levels from each connection contributing to the network.

Anatomical and diffusion processing pipelines to build the structural brain networks

Along with the MRI data, all the centres involved in this study provided the corresponding WM lesion segmentation mask for each subject. In PwMS where the lesion mask was outlined in T2 space, the centre provided the correspondent T2 image, which was subsequently registered to the T1w image using a rigid (6 DOF) transformation. These masks were used to obtain lesion-filled T1w images in order to guarantee accurate segmentation.¹⁵ We estimated normalised global brain and lesion volumes using the scaling factor from the FSL-SIENAX software (<https://fsl.fmrib.ox.ac.uk/fsl/fslwiki/SIENAX>) and harmonised these values through ComBat, including as a covariate MS phenotypes, to ensure that the biological variability related to the MS phenotypes is preserved while minimising the unwanted technical variability arising from centre effects.¹⁶ The lesion-filled T1w images were parcellated into 62 cortical and 14 subcortical GM regions using the anatomical Desikan-Killany atlas. The Mindboggle software (<https://mindboggle.info>), in conjunction with the Freesurfer and Advanced Normalization Tools (ANTs) packages, as well as the FSL-FIRST pipeline (<https://fsl.fmrib.ox.ac.uk/fsl/fslwiki/FIRST>), was employed in this analysis to generate regional volumes for cortical and subcortical areas. These regions were then used to define the network nodes.^{17,18}

To reduce the confounding effects derived from diffusion-weighted images (DWI) acquisition, a well-established DWI

preprocessing pipeline was followed using the FSL and MRtrix packages (<https://www.mrtrix.org/>), as described previously.¹⁹ These preprocessing steps involved skull stripping, Gibbs ringing correction, Marchenko-Pastur principal component analysis (MP-PCA) denoising, slice-wise outlier detection, eddy current and motion correction within DWI volumes (using FSL's eddy tool), rotation of the b-vectors, geometric distortion corrections depending on each dataset involved (gradient field maps, performing a non-linear registration of the b0 image to an undistorted T2 anatomical image or using a B0 undistorted synthetic image),^{20 21} and field bias correction. After these corrections, model fitting was performed on the undistorted DWI to estimate the diffusion tensor and then compute the quantitative FA scalar map using FSL's DTIFIT (<https://fsl.fmrib.ox.ac.uk/fsl/fslwiki/FDT/UserGuide>).²² In addition, the undistorted b0 images were used to improve the accuracy of DWI registration to the anatomical T1w images.

Quantitative FA connectivity matrices were obtained by performing constrained-spherical deconvolution and probabilistic advanced diffusion tractography.²³ A set of 6 million streamlines were generated into WM mask to capture the entire WM fibre trajectories, including both areas with lesions and without lesions, thereby mitigating the influence of reduced FA within lesions on the structural connectome reconstruction.⁶ This was achieved through the application of anatomically constrained tractography (five tissue types),²⁴ which established the assessment of 2850 WM connections based on all pairs of cortical and deep GM (dGM) regions. Subsequently, anatomical exclusion criteria were applied to reduce the number of spurious streamlines from each connection.²⁵ We defined pairs of GM regions as structurally connected if the connection was preserved after applying SIFT2 functions.²⁶ The mean FA along each reconstructed fibre pathway was computed to establish the whole-brain structural connectome between all pairs of GM regions. Finally, the connections that were present in less than 60% of the HCs group were removed from the network, ending up with 1818 connections, and we then corrected the effects of age and gender using linear regression.²⁷ As the FA-weighted adjacency matrices could suffer from intersite variability related to heterogeneity in the acquisition protocol, we harmonised the data with the ComBat model using an imputation technique for missing values.²⁸

Network metrics

Global and local network graph measures were estimated using the Brain Connectivity toolbox (<https://sites.google.com/site/bctnet/>).²⁹ We investigated local network measures like nodal strength (the sum of the edge weights connected to a node), nodal betweenness-centrality (the number of the shortest paths that pass through a node), nodal clustering coefficient (the fraction of the node's neighbours that are closed as triangles) and nodal local efficiency (the inverse of the shortest path distance between the nodes). In addition, we calculated the average of these local topological features for all the nodes involved in each network and the global efficiency to measure the global network properties.

Statistical analyses and classification tasks

A two-sample Student's t-test was carried out to assess differences in the network metrics and FA connectivity matrices between HCs and PwMS, as well as among different MS phenotypes. We applied multiple comparison tests with the Benjamini/Yekutieli method to control for false positives ($p < 0.05$) and only variables

with an effect size, measured using Cohen's D, greater than 0.6 in absolute value were considered for further statistical analysis.

We used a support vector machine classification algorithm to discern between the HCs and MS groups, and to classify the disease phenotypes using binary classification tasks once the significant graph-derived measures and the FA-weighted connections had been selected from the group differences. For this task, we analysed the receiver operating characteristic, while handling unbalanced data by subsampling the larger group in each comparison. Thus, our dataset for classification analysis varied depending on the smaller group analysed at each iteration. In each scenario, we used 75% of the dataset for training and 25% for validation purposes. Through a 10-fold cross-validation process applied to the entire selected dataset, we were able to determine the classification accuracy (F-measure) among MS subtypes. These models were also investigated using confusion matrices to assess other indicators of the classification's performance, such as precision, sensitivity and specificity. Finally, the 20 most important inter-regional connections were identified in each ML model proposed.

RESULTS

The clinical and demographic information was collected from the 823 PwMS (74 CIS, 571 RRMS, 121 SPMS and 57 PPMS) and 221 HCs included in the study. As expected, the PwMS with progressive forms of the disease were older and had higher scores on the Expanded Disability Status Scale, as well as a longer disease duration ($p < 0.05$). Lesion volume was larger in SPMS than in the other phenotypes, while normalised brain volume was smaller in SPMS and PPMS compared with the CIS and RRMS groups (table 1).

Network modifications in PwMS

When compared with HCs, the global network graph metrics (table 2) and local properties were significantly lower in all the PwMS. Moreover, PwMS presented a reduced FA in numerous connections (1686 of 1818 connections, 92.74%), with the strongest differences observed for the intrahemispheric and interhemispheric connections between regions connected to the cingulate, frontal, occipital and dGM structures, such as the right thalamus and right pallidum.

Network changes regarding MS phenotypes

There were similar disruptions to the global and regional properties of CIS (n=74) and RRMS (n=571) networks connections relative to the HCs, affecting 1454 (CIS, 79.98%) and 1484 (RRMS, 81.63%) of the 1818 connections. As no significant differences were found between these phenotypes, we combined them for the analyses (CIS/RRMS). There were significant differences in global (table 2, p values) and local graph network measures between SPMS and CIS/RRMS across all 76 brain network nodes, including strength, clustering coefficient and local efficiency. There was a lower FA in 1452 (79.87%) of the connections associated with the SPMS phenotype, involving bilateral areas of frontal, parietal, occipital and cingulate cortex, while higher FA values were found for two connections from the thalamus and left caudate relative to CIS/RRMS (figure 1A).

In comparison to CIS/RRMS, there were no statistically significant differences regarding global (table 2) and local graph measures in PPMS participants. At the same time, the PPMS phenotype was associated with significantly lower FA in 35 connections (1.92%), most of these involving the bilateral frontal and right parietal lobes or the insula, while there

Table 1 Characteristics of the sample

	HCS (n=221)	CIS (n=74)	RRMS (n=571)	SPMS (n=121)	PPMS (n=57)	P value HCS versus PwMS	P value MS types
Age, years	41.2 (30.3–49.7)	34.1 (28.9–42.3)	43 (35.9–50.6)	55.2 (49.5–61.5)	58.1 (50.5–65.8)	<0.001*	<0.001†
Female, n (%)	132 (60)	48 (65)	403 (71)	72 (60)	26 (46)	0.064‡	<0.001‡
Disease duration, years	–	0.3 (0.2–0.4)	9.8 (5.7–17.4)	20.1 (14.0–26.7)	16 (8.6–21.2)	–	<0.001†
EDSS	–	1.5 (0–5.5)	2.0 (0–7.5)	6.0 (1.5–8.0)	6.0 (2.5–8.0)	–	<0.001†
Normalised T2 lesion volume, cm ³	–	2.38 (0.7–4.9)	9.69 (4.4–17.7)	19.5 (7.3–34.3)	13.9 (4.4–24.1)	–	<0.001†
Normalised brain volum, cm ³	1504 (1434–1577)	1496 (1420–1570)	1464 (1402–1536)	1378 (1335–1420)	1413 (1333–1450)	<0.001*	<0.001†

The data represent the absolute numbers and the proportions of the qualitative data, or the median and IQR for the quantitative data.

*Wilcoxon signed-rank test.

†Kruskal-Wallis H test. Dunn’s test was used to analyse pairwise comparison between MS phenotypes: age and EDSS score were different in all PwMS groups except in the comparison between SPMS and PPMS, while disease duration was different in all groups. Additionally, the normalised T2 lesion volume exhibited differences when comparing CIS and RRMS to SPMS, as well as between PPMS and SPMS. Furthermore, the normalised brain volume demonstrated disparities between CIS and RRMS compared with SPMS and PPMS, and between PPMS and SPMS. All volumetric statistical analyses were performed after adjusting for age and sex, and applying the ComBat harmonisation.

‡ χ^2 test.

CIS, clinically isolated syndrome; EDSS, Expanded disability status scale; HCS, healthy controls; MS, multiple sclerosis; PPMS, primary progressive; PwMS, people with MS; RRMS, relapsing-remitting MS; SPMS, secondary-progressive.

was also a higher FA at 10 connections within the dGM or the left lateral and medial orbitofrontal cortical regions (figure 2). When comparing the global network properties of the progressive phenotypes, there were significant differences relative to the SPMS phenotype (table 2), with a weaker nodal strength at 55.3% of the nodes, lower local efficiency at 60.5% of the nodes and a lower clustering coefficient at 65.8% of the nodes in the SPMS phenotype, whereas there were no significant differences in the betweenness centrality measures. Moreover, there was a lower FA at 303 (16.70%) connections in the SPMS networks relative to the PPMS networks, mainly in the bilateral parietal and occipital cortex or the dGM (figure 1B).

Classification task according to MS disease and phenotype

The significant differences in the global and regional network characteristics between the phenotypes were used to distinguish PwMS from HCs, and to classify the disease courses. The accuracy of the models to discriminate PwMS from HCs based on FA connectivity matrices (81%) and on local properties (77%) was better than that of the model based on global network graphs (65%: table 3). The most informative connections to distinguish between PwMS and HCs included dGM structures, such as in the bilateral thalamus, hippocampus, putamen and caudate, or the right pallidum and cingulate regions.

Table 2 Global network measures

	HCS versus PwMS p value	CIS/RRMS versus SPMS p value	CIS/RRMS versus PPMS p value	SPMS versus PPMS p value
Strength	<0.001	<0.001	n.s	<0.001
Betweenness centrality	0.005	n.s	n.s	<0.001
Clustering coefficient	<0.001	<0.001	n.s	<0.001
Global efficiency	<0.001	<0.001	n.s	<0.001

CIS, clinically isolated syndrome; HCS, healthy controls; n.s., not significant; PPMS, primary progressive MS; RRMS, relapsing-remitting MS; SPMS, secondary-progressive MS.

The average accuracy in classifying the MS phenotypes was calculated based on the fraction of significant differences in the connections between CIS/RRMS and SPMS (71%), CIS/RRMS and PPMS (66%), and SPMS and PPMS (74%: figure 3 and table 3). As expected, the largest group CIS/RRMS was easier to identify correctly, while the other MS phenotypes were generally more difficult to discriminate with the classification models (see confusion matrix in figure 3A,B). The most important connections in the classification models could be identified (figure 4), and, the right thalamus, bilateral pallidum and left putamen being particularly important regions to differentiate CIS/RRMS from SPMS. The enhanced FA of the thalamic connections were those with the strongest weights. By contrast, areas of the frontal cortex enabled CIS/RRMS to be differentiated from PPMS, such as the left rostral and right caudal middle frontal cortex. Finally, both the left postcentral and parietal cortex (supramarginal and superior parietal) were the regions with the strongest weights to distinguish SPMS from PPMS. Nonetheless, the global and local graph-derived networks performed less accurately than using the FA-weighted connections itself when discriminating the MS subtypes (table 3).

DISCUSSION

In this study, we aimed to assess the clinical relevance of structural network measures in MS. We identified modifications to several components of brain networks that appear to be specific to different MS phenotypes. In PwMS, both the local and global graph properties of the networks and WM connections were altered, which in turn affects global network integrity. The network modifications associated with the CIS/RRMS and PPMS phenotypes are more similar, while SPMS showed stronger abnormalities relative to the other phenotypes. Classification algorithms were able to discriminate the MS phenotypes, with the best accuracy obtained when models use information from FA-weighted connections, especially those regarding thalamic connections, as opposed to those relying on graph metrics.

To address the current lack of knowledge on the value of structural network measures in MS, this multicentre study of advanced MRI data from a large cohort of subjects was designed

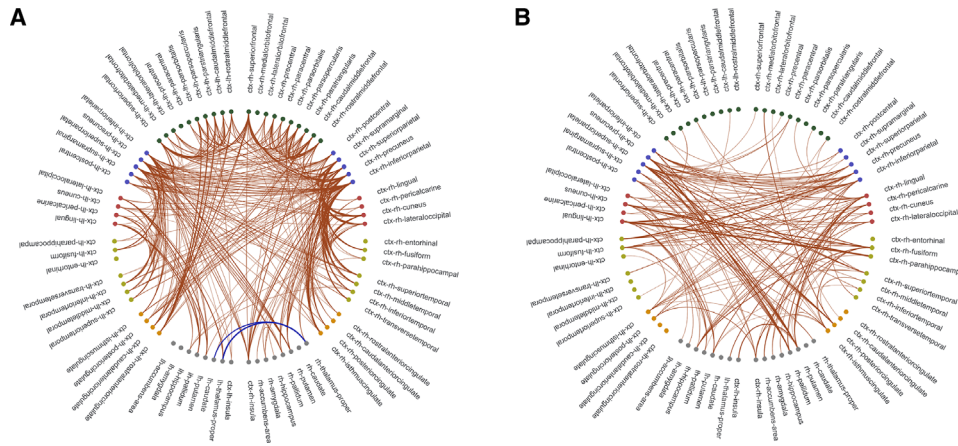


Figure 1 Connectograms comparing the MS phenotypes: (A) CIS/RRMS versus SPMS and (B) SPMS versus PPMS. Only differences with an effect size above 0.5 are shown (connections with a smaller FA in SPMS than in the other phenotypes are in red and those with a higher FA are in blue): These connectograms were generated using bokeh from Python V.3.7 (<http://bokeh.org/>). CIS, clinically isolated syndrome; ctx, cortex; FA, fractional anisotropy; lh, left hemisphere; MS, multiple sclerosis; PPMS, primary progressive MS; rh, right hemisphere; RRMS, relapsing-remitting MS; SPMS, secondary progressive MS.

to assess the diffusion-based structural connectivity characteristics of specific MS phenotypes. In the early stage of the disease, PwMS already express broad modifications to nodal and WM connectivity, triggering global network impairment. In later secondary progressive stages, the network modifications are more extensive, with widespread changes in connectivity associated with the SPMS phenotype.³⁰ Indeed, nearly 80% of connections in the SPMS group had a lower FA than in CIS/RRMS, mainly involving bilateral areas of the frontal, parietal and temporal cortex. These results reflect the severe diffuse WM

damage at advanced stages of the disease, with higher lesion load, where more normal-appearing WM damage and more cortical atrophy are usually evident, leading to a prominent disconnection syndrome.^{31 32} By contrast, the PPMS phenotype differed less from CIS/RRMS, with alterations limited to bilateral frontal and right parietal connections, and less extensive network changes than in SPMS, as suggested previously.³³ These findings are concordant with what is commonly observed in PPMS, and with the present results, where the burden of brain lesions is lower and atrophy predominates (table 1).³⁴ All in all, these results support the idea that MS phenotypes reflect a continuum of pathological mechanisms underlying the disease course, suggesting that the observed microstructural differences across subtypes represent varying degrees of damage and inflammation along the progression of a single disease process rather than discrete, separable phenotypes.

One interesting finding was that the FA of some connections from the thalamus and other dGM structures was higher in SPMS and PPMS than in CIS/RRMS, although the FA values did not reach the values of the HCs. Indeed, atrophy of the thalamus is an early finding in MS,³⁵ although silent neurodegeneration at

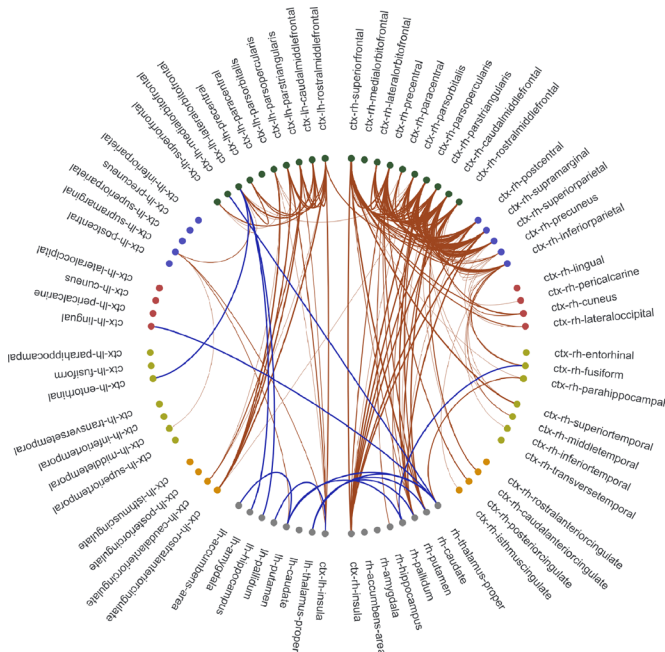


Figure 2 Comparison of the MS connectograms from CIS/RRMS and PPMS. All the significant differences are shown (with a smaller FA in PPMS relative to CIS/RRMS in red and a higher FA in blue): These connectograms were generated using bokeh from Python V.3.7 (<http://bokeh.org/>). CIS, clinically isolated syndrome; ctx, cortex; FA, fractional anisotropy; lh, left hemisphere; MS, multiple sclerosis; PPMS, primary progressive MS; rh, right hemisphere; RRMS, relapsing-remitting MS; SPMS, secondary progressive MS.

Table 3 Classification measures from super vector machine algorithms to discriminate groups of participants

		Hcs versus PwMS	CIS/RRMS versus SPMS	CIS/RRMS versus PPMS	SPMS versus PPMS
Global graph metrics	Accuracy	65%±4%	65%±7%	n.a.	55%±8%
	Precision	60%±6%	60%±11%	n.a.	57%±11%
	Recall	71%±2%	71%±3%	n.a.	54%±6%
Local graph metrics	Accuracy	77%±3%	60%±5%	n.a.	56%±8%
	Precision	77%±3%	59%±4%	n.a.	54%±8%
	Recall	77%±3%	62%±8%	n.a.	59%±8%
FA of connections	Accuracy	81%±4%	71%±7%	66%±4%	74%±5%
	Precision	81%±4%	66%±10%	63%±5%	66%±8%
	Recall	80%±4%	77%±6%	71%±8%	85%±4%

Classification algorithms could not be applied to metrics that did not show significant differences in the group analyses. CIS, clinically isolated syndrome; HCs, healthy controls; n.a., not be applied; PPMS, primary progressive MS; PwMS, people with MS; RRMS, relapsing-remitting MS; SPMS, secondary progressive MS.

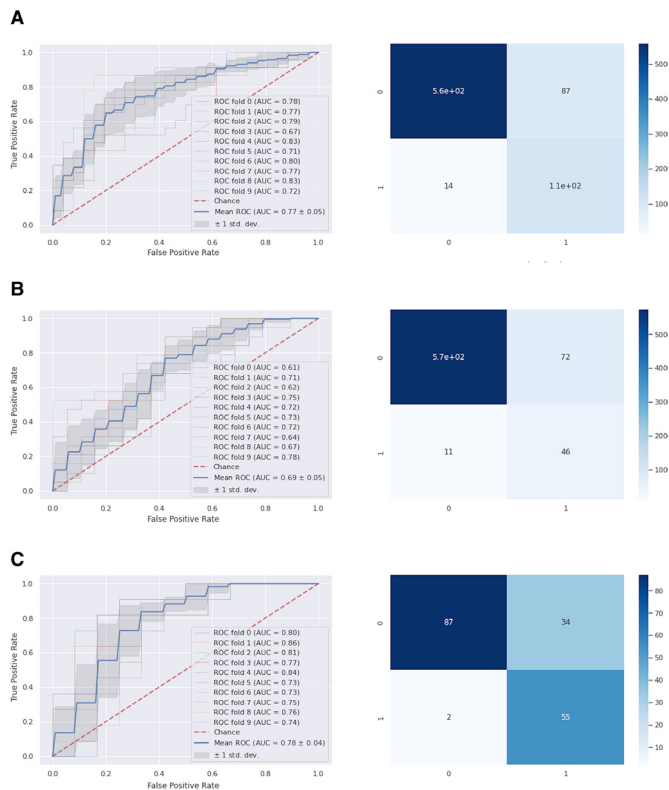


Figure 3 Performance of the classification models for the MS phenotypes and confusion matrices. The receiver operating characteristics (ROC) curves were generated to evaluate the classification performance between (A) CIS/RRMS versus SPMS, (B) CIS/RRMS versus PPMS and (C) SPMS versus PPMS. AUC, area under the curve; CIS, clinically isolated syndrome; MS, multiple sclerosis; PPMS, primary progressive MS; RRMS, relapsing-remitting MS; SPMS, secondary progressive MS.

a microstructural level in subcortical projection systems occurs in even earlier stages of the disease.³⁶ In progressive forms of MS, changes in neuronal micro-organisation occur in conjunction with severe atrophy. Therefore, the significant increase in FA at later phases might be related to tighter packing of WM fibres, which leads to an increase in myelin density and reduces fibre dispersion.³⁷

We analysed the value of features of structural connectivity to differentiate PwMS from healthy individuals and to discern between clinical phenotypes. The resulting ML models demonstrated an accuracy of up to 81% in distinguishing between PwMS and HCs, also identifying the most relevant structural changes in connections from the cingulate cortex and dGM structures like the thalamus and pallidum, areas known for their strong clinical correlations with disability and cognition.^{4 38} The capacity to classify MS phenotypes based on FA-weighted measures was reflected by accuracy values between 66% and 74%, with the greatest accuracy observed in ML models to discern the SPMS phenotype from the others. Nevertheless, the superior discriminative ability of FA-weighted connectivity matrices compared with graph network measures implies that converting the former to the latter may result in the loss of important information. In addition, the most relevant structural connectivity patterns to classify MS subtypes differed depending on the phenotypes compared. Thus, dGM regions were the most relevant to differentiate CIS/RRMS from SPMS, especially these connections involving the thalamus and pallidum. Connections from the parietal cortex (bilateral postcentral and superior parietal) and

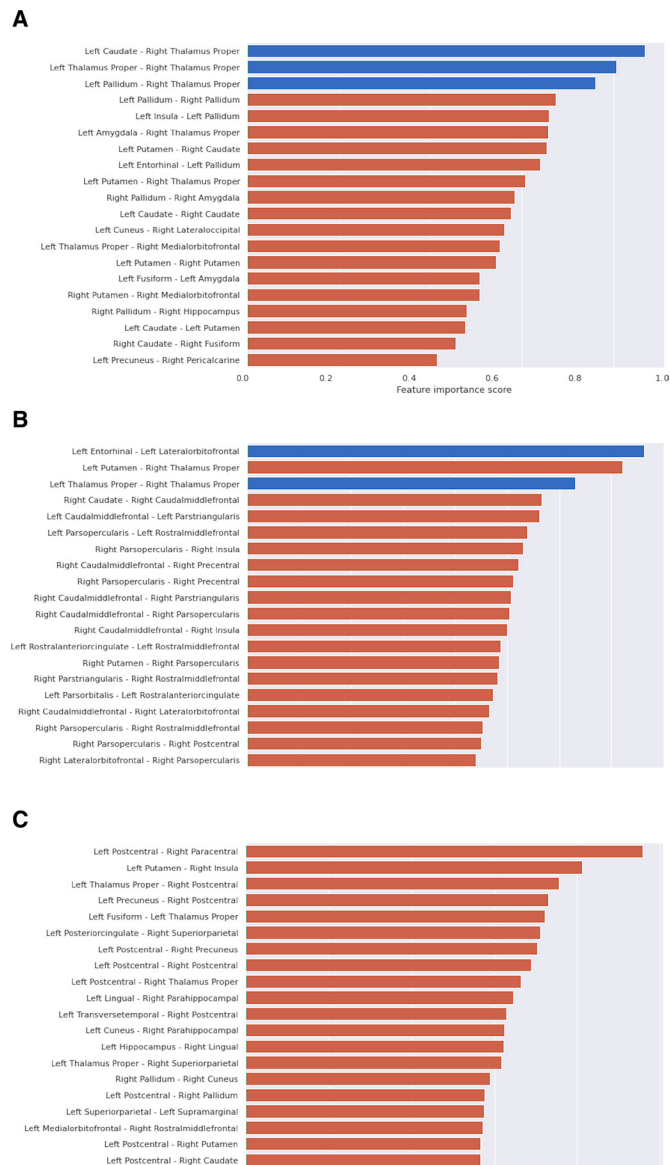


Figure 4 The most important connections established by the machine learning model to discriminate MS phenotypes based on FA: (A) CIS/RRMS versus SPMS; (B) CIS/RRMS versus PPMS and (C) SPMS versus PPMS. The weights were normalised according to the highest values, with red bars representing lower FA connection weights and blue bars representing higher weights. CIS, clinically isolated syndrome; FA, fractional anisotropy; MS, multiple sclerosis; PPMS, primary progressive MS; RRMS, relapsing-remitting MS; SPMS, secondary progressive MS.

thalamus were the most relevant to differentiate SPMS from PPMS, while tracts involving the frontal cortex (pars opercularis, caudal and rostral middle frontal) were crucial in distinguishing CIS/RRMS from PPMS. Our findings support previous studies on smaller cohorts that reported good discrimination of clinical MS phenotypes using ML-based classification methods and deep learning architectures,^{13 14 39} providing evidence of the distinct patterns of WM connectivity in MS.

There are some limitations to this study that should be noted. The dataset was collected at eight MAGNIMS sites that had some heterogeneity in the acquisition protocols, the number of participants and the representation of phenotypes. Thus, we applied the ComBat approach to diminish the individual site effects while preserving the interindividual FA variability.¹⁶ The low number of

PPMS patients included, which is concordant with the frequency of this phenotype in the disease could have limited the power to detect subtle differences. Quantitative FA metrics may be influenced by the spatial configuration of the tissue, such as the crossing fibres, which can limit its pathological specificity.⁴⁰ Hence, further studies with advanced multicompartmental diffusion methods could help to overcome this limitation and provide a better understanding of the pathological mechanisms underlying the network changes. Finally, future research involving functional connectivity and longitudinal network studies is warranted to gain a more comprehensive understanding of the relationship between structural disconnection and functional reorganisation.

In conclusion, structural brain connectivity is disrupted globally in PwMS and differential patterns of regional WM changes are specific to MS phenotypes. As such, CIS/RRMS and PPMS have similar network modifications, while SPMS is associated with more widespread changes in connectivity relative to other phenotypes. Classification methods can distinguish between phenotypes and the largest discriminative value is obtained by considering the integrity of the subcortical connections.

Author affiliations

¹Neuroimmunology and Multiple Sclerosis Unit and Laboratory of Advanced Imaging in Neuroimmunological Diseases (ImaginEM), Hospital Clinic and Institut d'Investigacions Biomèdiques August Pi i Sunyer (IDIBAPS), University of Barcelona, Barcelona, Spain

²MS Center Amsterdam, Anatomy and Neurosciences, Vrije Universiteit Amsterdam, Amsterdam Neuroscience, Amsterdam UMC location VUmc, Amsterdam, The Netherlands

³MS Center Amsterdam, Neurology, Vrije Universiteit Amsterdam, Amsterdam Neuroscience, Amsterdam UMC location VUmc, Amsterdam, The Netherlands

⁴Radiology and Nuclear Medicine, Vrije Universiteit Amsterdam, Amsterdam Neuroscience, Amsterdam UMC location VUmc, Amsterdam, The Netherlands

⁵Queen Square Institute of Neurology and Centre for Medical Image Computing, University College London, London, UK

⁶Neuroimaging Research Unit, Institute of Experimental Neurology, Division of Neuroscience, IRCCS San Raffaele Scientific Institute, Milano, Italy

⁷Neurology Unit, IRCCS San Raffaele Scientific Institute, Milano, Italy

⁸Vita-Salute San Raffaele University, Milano, Italy

⁹Neurophysiology Service, IRCCS San Raffaele Scientific Institute, Milano, Italy

¹⁰Department of Neurology, Neurostimulation and Neuroimaging, Focus Program Translational Neuroscience (FTN), Rhine Main Neuroscience Network (rmn2), University Medical Center of the Johannes Gutenberg University, Mainz, Germany

¹¹Mental Health and Clinical Neuroscience, School of Medicine, University of Nottingham, Nottingham, UK; and NIHR Nottingham Biomedical Research Centre, Nottingham, UK

¹²Institute of Neuroradiology, St. Josef Hospital, Ruhr-University Bochum, Bochum, Germany

¹³Section of Neuroradiology, Department of Radiology, Vall d'Hebron University Hospital and Research Institute (VHIR), Barcelona, Spain

¹⁴Neurology-Neuroimmunology Department, Centre d'Esclerosi Múltiple de Catalunya (Cemcat), Vall d'Hebron Barcelona Hospital Campus, Barcelona, Spain

¹⁵Queen Square MS Centre, Department of Neuroinflammation, UCL Queen Square Institute of Neurology, Faculty of Brain Science, University College of London, London, UK

¹⁶Centre for Medical Image Computing (CMIC), Department of Medical Physics and Bioengineering, University College London, London, UK

¹⁷E-health Centre, Universitat Oberta de Catalunya, Barcelona, Spain

Twitter Eva M Strijbis @Eef111, Jaume Sastre-Garriga @J_SastreGarriga and Sara Collorone @SaraCollorone

Contributors SL: designed and conceptualised study; major role in acquisition of data; analysed and interpreted the data; drafted and revised the manuscript for intellectual content; had full access to all the data in the study and takes responsibility as guarantor for the integrity of the data and the accuracy of the data analysis. EM-H, ES, FV: major role in acquisition of data; analysed and interpreted the data; drafted and revised the manuscript for intellectual content. EL-S, AC, SA-A, MMS, EMS, HV, FB, MAR, MF, EP, SG, VF, RAD, BB, CL, DP, AR, JSG, SC, FP, AT, OC, AS, YB: acquisition of data; analysed and interpreted the data; revised the manuscript for intellectual content.

Funding This work was sponsored by the Instituto Carlos III (ISCIII) and co-funded by the European Union through the Plan Estatal de Investigación Científica y

Técnica y de Innovación 2015-2024 (PI15/00587 to SL, and AS; PI18/01030 to SL and AS; PI21/01189 to SL and AS), by the Red Española de Esclerosis Múltiple (REEM-RD16/0015/0002, RD16/0015/0003). Part of this work was supported by the German Federal Ministry for Education and Research, BMBF, German Competence Network Multiple Sclerosis (KKNMS), grants 01G116011 and 01G10914. The authors are grateful to the IDIBAPS Magnetic resonance imaging platform for their support. This work was partially developed at the building Centro Esther Koplowitz, Barcelona, CERCA Programme/Generalitat de Catalunya.

Disclaimer The funding bodies had no role in the design and performance of the study; the collection, management, analysis and interpretation of the data; the preparation, revision or approval of the manuscript; and the decision to submit the manuscript for publication.

Competing interests ES and EL-S received travel reimbursement from Sanofi and ECTRIMS; AC received support from the ECTRIMS-MAGNIMS fellowship (2018) and, was granted a postdoctoral fellowship from ECTRIMS in 2022; AS received compensation for consulting services and speaker honoraria from Merck, Biogen-Idec, Sanofi, Novartis, Roche, Janssen and Horizon Therapeutics; YB received speaking honoraria from Biogen, Novartis and Genzyme; SL received compensation for consulting services and speaker honoraria from Biogen Idec, Novartis, TEVA, Genzyme, Sanofi and Merck. MMS serves on the editorial board of Neurology and Frontiers in Neurology, receives research support from the Dutch MS Research Foundation, Eurostars-EUREKA, ARSEP, Amsterdam Neuroscience, MAGNIMS and ZonMW and has served as a consultant for or received research support from Atara Biotherapeutics, Biogen, Celgene/Bristol Myers Squibb, Genzyme, MedDay and Merck. HV has received research grants from Pfizer, Merck Serono, Novartis, and Teva; speaker honoraria from Novartis; and consulting fees from Merck Serono, all paid directly to his institution. FB: Steering committee and iDMC member for Biogen, Merck, Roche, Eisai. Consultant for Roche, Biogen, Merck, IXICO, Jansen, Combinostics. Research agreements with Novartis, Merck, Biogen, GE, Roche. Co-founder and shareholder of Queen Square Analytics LTD. MAR received speaker honoraria from Bayer, Biogen, Bristol Myers Squibb, Celgene, Genzyme, Merck Serono, Novartis, Roche, and Teva and research support from the Canadian MS Society and Fondazione Italiana Sclerosi Multipla. MF is editor-in-chief of the Journal of Neurology and Associate Editor of Human Brain Mapping, Neurological Sciences, and Radiology, received compensation for consulting services and/or speaking activities from Alexion, Ammiral, Bayer, Biogen, Celgene, Eli Lilly, Genzyme, Merck-Serono, Novartis, Roche, Sanofi, Takeda, and Teva Pharmaceutical Industries, and receives research support from Biogen Idec, Merck-Serono, Novartis, Roche, Teva Pharmaceutical Industries, the Italian Ministry of Health, Fondazione Italiana Sclerosi Multipla, and ARiSLA (Fondazione Italiana di Ricerca per la SLA). BB received financial support by the German Federal Ministry for Education and Research, BMBF, German Competence Network Multiple Sclerosis (KKNMS), grant no.01G116011. CL received a research grant by the German Federal Ministry for Education and Research, BMBF, German Competence Network Multiple Sclerosis (KKNMS), grant no.01G116011, has received consulting and speaker's honoraria from Biogen Idec, Bayer Schering, Daiichi Sanykyo, Merck Serono, Novartis, Sanofi, Genzyme and TEVA. AR serves on scientific advisory boards for Novartis, Sanofi-Genzyme, Synthetic MR, TensorMedical, Roche, Biogen, and OLEA Medical, and has received speaker honoraria from Bayer, Sanofi-Genzyme, Merck-Serono, Teva Pharmaceutical Industries, Novartis, Roche, Bristol-Myers and Biogen. JS-G serves as co-editor for Europe on the editorial board of Multiple Sclerosis Journal and as editor-in-chief in Revista de Neurología, receives research support from Fondo de Investigaciones Sanitarias (19/950) and has served as a consultant/speaker for Biogen, Celgene/Bristol Myers Squibb, Genzyme, Novartis, Merck and Roche. AT has been supported by grants from MRC (MR/S026088/1), NIHR BRC (541/CAP/OC/818837) and RoseTrees Trust (A1332 and PGL21/10079), has had meeting expenses from Merck, Biomedica and Biogen Idec and was UK PI for two clinical trials sponsored by MEDDAY (MS-ON-NCT02220244 and MS-SPI2-NCT02220244). OC acts as a consultant for Novartis and Merck, and has received research funding from: NIHR, UK MS Society, NIHR UCLH BRC, MRC, Rosetrees Trust.

Patient consent for publication Not applicable.

Ethics approval This study involves human participants and the ethical review board at the Hospital Clinic in Barcelona (HCB) granted approval for the MAGNIMS connectivity project, and all participants provided written consent for the use of their data. The Clinical Research Ethics Committee (CEIC) identification number for this study is HCB/2017/0836. Participants gave informed consent to participate in the study before taking part.

Provenance and peer review Not commissioned; externally peer reviewed.

Data availability statement Data are available on reasonable request.

Supplemental material This content has been supplied by the author(s). It has not been vetted by BMJ Publishing Group Limited (BMJ) and may not have been peer-reviewed. Any opinions or recommendations discussed are solely those of the author(s) and are not endorsed by BMJ. BMJ disclaims all liability and responsibility arising from any reliance placed on the content. Where the content

includes any translated material, BMJ does not warrant the accuracy and reliability of the translations (including but not limited to local regulations, clinical guidelines, terminology, drug names and drug dosages), and is not responsible for any error and/or omissions arising from translation and adaptation or otherwise.

ORCID iDs

Eloy Martinez-Heras <http://orcid.org/0000-0001-9937-3162>
 Alberto Calvi <http://orcid.org/0000-0002-1953-2803>
 Menno M Schoonheim <http://orcid.org/0000-0002-2504-6959>
 Eva M Strijbis <http://orcid.org/0000-0001-6705-5864>
 Maria A Rocca <http://orcid.org/0000-0003-2358-4320>
 Massimo Filippi <http://orcid.org/0000-0002-5485-0479>
 Sergiu Groppa <http://orcid.org/0000-0002-2551-5655>
 Vinzenz Fleischer <http://orcid.org/0000-0002-3293-5121>
 Robert A Dineen <http://orcid.org/0000-0002-9523-2546>
 Alex Rovira <http://orcid.org/0000-0002-2132-6750>
 Jaume Sastre-Garriga <http://orcid.org/0000-0002-1589-2254>
 Sara Collorone <http://orcid.org/0000-0003-1506-8983>
 Sara Llufriu <http://orcid.org/0000-0003-4273-9121>

REFERENCES

- Rocca MA, Amato MP, De Stefano N, et al. Clinical and imaging assessment of cognitive dysfunction in multiple sclerosis. *The Lancet Neurology* 2015;14:302–17.
- Thompson AJ, Banwell BL, Barkhof F, et al. Diagnosis of multiple sclerosis: 2017 revisions of the McDonald criteria. *The Lancet Neurology* 2018;17:162–73.
- Granziera C, Wuerfel J, Barkhof F, et al. Quantitative magnetic resonance imaging towards clinical application in multiple sclerosis. *Brain* 2021;144:1296–311.
- Llufriu S, Martinez-Heras E, Solana E, et al. Structural networks involved in attention and executive functions in multiple sclerosis. *Neuroimage Clin* 2017;13:288–96.
- Filippi M, Brück W, Chard D, et al. Association between pathological and MRI findings in multiple sclerosis. *Lancet Neurol* 2019;18:198–210.
- Solana E, Martinez-Heras E, Martinez-Lapiscina EH, et al. Magnetic resonance markers of tissue damage related to connectivity disruption in multiple sclerosis. *Neuroimage Clin* 2018;20:161–8.
- Shu N, Duan Y, Huang J, et al. Progressive brain rich-club network disruption from clinically isolated syndrome towards multiple sclerosis. *Neuroimage Clin* 2018;19:232–9.
- Fleischer V, Radetz A, Ciolac D, et al. Graph theoretical framework of brain networks in multiple sclerosis: a review of concepts. *Neuroscience* 2019;403:35–53.
- Charalambous T, Tur C, Prados F, et al. Structural network disruption markers explain disability in multiple sclerosis. *J Neurol Neurosurg Psychiatry* 2019;90:219–26.
- Koubyr I, Deloire M, Besson P, et al. Longitudinal study of functional brain network reorganization in clinically isolated syndrome. *Mult Scler* 2020;26:188–200.
- Schoonheim MM, Meijer KA, Geurts JGG. Network collapse and cognitive impairment in multiple sclerosis. *Front Neurol* 2015;6:82.
- Pagani E, Rocca MA, De Meo E, et al. Structural connectivity in multiple sclerosis and modeling of disconnection. *Mult Scler* 2020;26:220–32.
- Kocevar G, Stamile C, Hannou S, et al. Graph theory-based brain connectivity for automatic classification of multiple sclerosis clinical courses. *Front Neurosci* 2016;10:478.
- Marzullo A, Kocevar G, Stamile C, et al. Classification of multiple sclerosis clinical profiles via graph convolutional neural networks. *Front Neurosci* 2019;13:594.
- Battaglini M, Jenkinson M, De Stefano N. Evaluating and reducing the impact of white matter lesions on brain volume measurements. *Hum Brain Mapp* 2012;33:2062–71.
- Fortin J-P, Cullen N, Sheline YI, et al. Harmonization of cortical thickness measurements across scanners and sites. *Neuroimage* 2018;167:104–20.
- Klein A, Ghosh SS, Bao FS, et al. Mindboggling morphometry of human brains. *PLoS Comput Biol* 2017;13:e1005350.
- Patenaude B, Smith SM, Kennedy DN, et al. A Bayesian model of shape and appearance for subcortical brain segmentation. *Neuroimage* 2011;56:907–22.
- Tournier J-D, Smith R, Raffelt D, et al. MRtrix3: a fast, flexible and open software framework for medical image processing and visualisation. *Neuroimage* 2019;202:116137.
- Schilling KG, Blaber J, Huo Y, et al. Synthesized B0 for diffusion distortion correction (Synb0-DisCo). *Magnetic Resonance Imaging* 2019;64:62–70.
- Tao R, Fletcher PT, Gerber S, et al. A variational image-based approach to the correction of susceptibility artifacts in the alignment of diffusion weighted and structural MRI. *Inf Process Med Imaging* 2009;21:664–75.
- Basser PJ, Mattiello J, LeBihan D. MR diffusion tensor spectroscopy and imaging. *Biophys J* 1994;66:259–67.
- Jeurissen B, Tournier J-D, Dhollander T, et al. Multi-tissue constrained spherical deconvolution for improved analysis of multi-shell diffusion MRI data. *Neuroimage* 2014;103:411–26.
- Smith RE, Tournier J-D, Calamante F, et al. Anatomically-constrained tractography: improved diffusion MRI streamlines tractography through effective use of anatomical information. *Neuroimage* 2012;62:1924–38.
- Martinez-Heras E, Varriano F, Prčková V, et al. Improved framework for tractography reconstruction of the optic radiation. *PLoS One* 2015;10:e0137064.
- Smith RE, Tournier J-D, Calamante F, et al. SIFT2: enabling dense quantitative assessment of brain white matter connectivity using streamlines tractography. *Neuroimage* 2015;119:338–51.
- Solana E, Martinez-Heras E, Casas-Roma J, et al. Modified connectivity of vulnerable brain nodes in multiple sclerosis, their impact on cognition and their discriminative value. *Sci Rep* 2019;9:20172.
- Radua J, Vieta E, Shinohara R, et al. Increased power by harmonizing structural MRI site differences with the combat batch adjustment method in ENIGMA. *Neuroimage* 2020;218:116956.
- Rubinov M, Sporns O. Complex network measures of brain connectivity: uses and interpretations. *Neuroimage* 2010;52:1059–69.
- Collorone S, Prados F, Hagens MH, et al. Single-subject structural cortical networks in clinically isolated syndrome. *Mult Scler* 2020;26:1392–401.
- He Y, Dagher A, Chen Z, et al. Impaired small-world efficiency in structural cortical networks in multiple sclerosis associated with white matter lesion load. *Brain* 2009;132:3366–79.
- Steenwijk MD, Daams M, Pouwels PJW, et al. Unraveling the relationship between regional gray matter atrophy and pathology in connected white matter tracts in long-standing multiple sclerosis. *Hum Brain Mapp* 2015;36:1796–807.
- Preziosa P, Rocca MA, Mesaros S, et al. Intrinsic damage to the major white matter tracts in patients with different clinical phenotypes of multiple sclerosis: a voxelwise diffusion-Tensor MR study. *Radiology* 2011;260:541–50.
- Siger M. Magnetic resonance imaging in primary progressive multiple sclerosis patients: review. *Clin Neuroradiol* 2022;32:625–41.
- Eshaghi A, Prados F, Brownlee WJ, et al. Deep gray matter volume loss drives disability worsening in multiple sclerosis. *Ann Neurol* 2018;83:210–22.
- Deppe M, Krämer J, Tenberge J-G, et al. Early silent microstructural degeneration and atrophy of the thalamocortical network in multiple sclerosis. *Hum Brain Mapp* 2016;37:1866–79.
- Andersen KW, Lasič S, Lundell H, et al. Disentangling white-matter damage from physiological fibre orientation dispersion in multiple sclerosis. *Brain Commun* 2020;2:fcaa077.
- Dineen RA, Vilisaar J, Hlinka J, et al. Disconnection as a mechanism for cognitive dysfunction in multiple sclerosis. *Brain* 2009;132:239–49.
- Zurita M, Montalba C, Labbé T, et al. Characterization of relapsing-remitting multiple sclerosis patients using support vector machine classifications of functional and diffusion MRI data. *Neuroimage Clin* 2018;20:724–30.
- Martinez-Heras E, Grussu F, Prados F, et al. Diffusion-weighted imaging: recent advances and applications. *Semin Ultrasound CT MR* 2021;42:490–506.